AD-A170 982 AERODYNAMIC BREAKUP OF POLYMER SOLUTIONS VIA DIGITAL IMAGE PROCESSING TECHNIQUES(U) JET PROPULSION LAB PASADENA CA M A HERNAN ET AL. APR 86 CRDEC-CR-86020 1/1

UNCLASSIFIED MIPR-23111-1249 F/G 20/4 NL

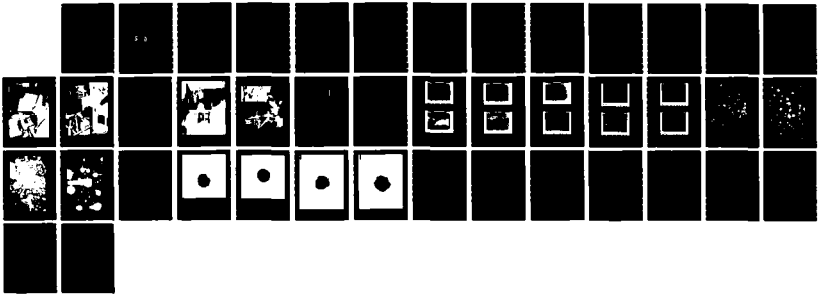

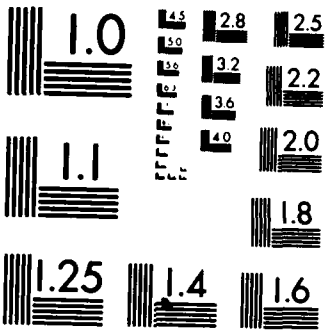

(12)



CHEMICAL RESEARCH, DEVELOPMENT & ENGINEERING CENTER

CRDEC-CR-86020

# AERODYNAMIC BREAKUP OF POLYMER SOLUTIONS VIA DIGITAL IMAGE PROCESSING TECHNIQUES



by M.A. Hernan
P. Parikh
A. Yavrouian
V. Sarohia

JET PROPULSION LABORATORY
Pasadena, CA 91109

April 1986



U.S. ARMY ARMAMENT MUNITIONS CHEMICAL COMMAND

Aberdeen Proving Ground, Maryland 21010-5423

## Disclaimer

The findings in this report are not to be construed as an official Department of the Army position unless so designated by other authorizing documents.

## Destruction Notice

For classified documents, follow the procedures in DoD 5200.22-M, Industrial Security Manual, Section II-19, or DoD 5200.1-R, Information Security Program Regulation, Chapter IX. For unclassified, limited documents, destroy by any method that will prevent disclosure of contents or reconstruction of the document.

## Distribution Statement

Approved for public release; distribution is unlimited.

UNCLASSIFIED
SECURITY CLASSIFICATION OF THIS PAGE

AD-A170 982

# REPORT DOCUMENTATION PAGE

| | |
|---|---|
| 1a REPORT SECURITY CLASSIFICATION<br>UNCLASSIFIED | 1b RESTRICTIVE MARKINGS |
| 2a SECURITY CLASSIFICATION AUTHORITY | 3 DISTRIBUTION / AVAILABILITY OF REPORT<br>Approved for public release; distribution is unlimited. |
| 2b DECLASSIFICATION / DOWNGRADING SCHEDULE | |
| 4 PERFORMING ORGANIZATION REPORT NUMBER(S)<br>CRDEC-CR-86020 | 5 MONITORING ORGANIZATION REPORT NUMBER(S) |
| 6a NAME OF PERFORMING ORGANIZATION<br>Jet Propulsion Laboratory<br>6b OFFICE SYMBOL (If applicable) | 7a NAME OF MONITORING ORGANIZATION |
| 6c ADDRESS (City, State, and ZIP Code)<br>4800 Oak Grove Drive<br>Pasadena, CA 91109 | 7b ADDRESS (City, State, and ZIP Code) |
| 8a NAME OF FUNDING / SPONSORING ORGANIZATION<br>CRDEC<br>8b OFFICE SYMBOL (If applicable)<br>SMCCR-RSC-P | 9 PROCUREMENT INSTRUMENT IDENTIFICATION NUMBER<br>ARRADCOM* MIPR 23111-1249 |
| 8c ADDRESS (City, State, and ZIP Code)<br>Aberdeen Proving Ground, MD 21010-5423 | 10 SOURCE OF FUNDING NUMBERS<br>PROGRAM ELEMENT NO. / PROJECT NO. / TASK NO. / WORK UNIT ACCESSION NO |

11 TITLE (Include Security Classification)
Aerodynamic Breakup of Polymer Solutions via Digital Image Processing Techniques

12 PERSONAL AUTHOR(S)
Hernan, M.A., Parikh, P., Yavrouian, A., and Sarohia, V.

| 13a TYPE OF REPORT | 13b TIME COVERED | 14 DATE OF REPORT (Year, Month, Day) | 15 PAGE COUNT |
|---|---|---|---|
| Contractor | FROM 82 NOV TO 85 JUN | 1986 April | 39 |

16 SUPPLEMENTARY NOTATION
Contract Officer's Representative: Vincent McHugh, SMCCR-RSC-P, (301) 671-2721/4125
*ARRADCOM is now the U.S. Army Armament Research, Development and Engineering Center (ARDEC)

| 17 COSATI CODES | | | 18 SUBJECT TERMS (Continue on reverse if necessary and identify by block number) |
|---|---|---|---|
| FIELD | GROUP | SUB-GROUP | Aerodynamic Breakup, Polymer Solution, and Digital Imaging Analysis |
| 07 | 04 | | |
| 14 | 02 | | |

19 ABSTRACT (Continue on reverse if necessary and identify by block number)

The behavior of viscoelastic polymer solutions when exposed to high velocity airstream have been experimentally investigated. High speed pulsed laser photographic and digital image enhancement techniques have been used to visualize and characterize in-flight breakup of polymer solutions. Experiments with several polymer concentrations and various temperatures have been conducted in two facilities. The first set-up utilizes a high speed, free-jet flow and provides initial transient breakup behavior. Increased flight time for polymer relaxation was achieved by a unique co-flowing jet-facility developed for this task. Limited data obtained on this set-up are also presented.

| 20 DISTRIBUTION / AVAILABILITY OF ABSTRACT | 21 ABSTRACT SECURITY CLASSIFICATION |
|---|---|
| ☒ UNCLASSIFIED/UNLIMITED ☐ SAME AS RPT ☐ DTIC USERS | UNCLASSIFIED |

| 22a NAME OF RESPONSIBLE INDIVIDUAL | 22b TELEPHONE (Include Area Code) | 22c OFFICE SYMBOL |
|---|---|---|
| TIMOTHY E. HAMPTON | (301) 671-2914 | SMCCR-SPD-R |

DD FORM 1473, 84 MAR 83 APR edition may be used until exhausted
All other editions are obsolete.

SECURITY CLASSIFICATION OF THIS PAGE
UNCLASSIFIED

17. COSATI Codes (Continued)

| Group | Field |
|---|---|
| 20 | 04 |

## PREFACE

The work described in this report was authorized under Contract No. ARRADCOM* MIPR 23111-1249. This work was started in November 1982 and completed in June 1985.

The use of trade names or manufacturers' names in this report does not constitute an official endorsement of any commercial products. This report may not be cited for purposes of advertisement.



This document has been approved for release to the public.

### Acknowledgments

The research described in this report was carried out by the Jet Propulsion Laboratory, California Institute of Technology, and was sponsored by the U.S. Army Chemical Research, Development and Engineering Center (CRDEC), Aberdeen Proving Ground, Maryland. The authors benefitted throughout this program from the technical discussions with Dr. Wendel Shuely of CRDEC. The help of Mr. Robert Smither and Mr. Wayne Bixler in construction and acquiring of the experimental data is greatly appreciated.



*This work was begun before the U.S. Army Armament Research and Development Command (ARRADCOM) became the U.S. Army Armament Research, Development and Engineering Center (ARDEC).

BLANK

## TABLE OF CONTENTS


| | | Page |
|---|---|---|
| 1. | INTRODUCTION | 9 |
| 2. | EXPERIMENTAL APPROACH | 9 |
| | 2.1 Test Fluids | 9 |
| | 2.2 Wind Tunnel Test Procedure | 10 |
| | 2.2.1 Open Jet Wind Tunnel | 10 |
| | 2.2.2 Coaxial Jet Facility | 10 |
| | 2.3 Flow Illumination and Photographic Techniques | 10 |
| | 2.4 Digital Image Analysis | 17 |
| 3. | RESULTS AND DISCUSSIONS | 17 |
| | 3.1 Free Jet | 17 |
| | 3.2 Coaxial Jet | 27 |
| 4. | CONCLUSIONS | 27 |
| | LITERATURE CITED | 35 |
| | Appendix - Image Processing System Description | 37 |
| | A.1 System Architecture | 37 |
| | A.2 Software Description | 37 |

## LIST OF FIGURES


| Figure | | Page |
|---|---|---|
| 1 | Free-Jet Facility. | 11 |
| 2 | Free-Jet Facility. | 12 |
| 3 | Sketch of Coaxial Jet Facility. | 13 |
| 4 | Coaxial Jet Facility. | 14 |
| 5 | Close-up of Coaxial Jet Facility. | 15 |
| 6 | Schematic of Background Illustration and Photographic Technique. | 16 |
| 7 | Image Enhanced Breakup of Glycerol. | 18 |
| 8 | Near-Field Breakup of 0.5% Polymer Solution. | 18 |
| 9 | Near-Field Breakup of 1% Polymer Solution. | 19 |
| 10 | Near-Field Breakup of 2% Polymer Solution. | 20 |
| 11 | Near-Field Breakup of 5% Polymer Solution. | 20 |
| 12 | Influence of Temperature on Near-Field Breakup of 5% Polymer Solution. | 22 |
| 13 | Impressions of 0.5% Polymer Solution Breakup at Temperature 20$^{o}$C, Freestream Velocity 250 m/s, and 12m Downstream from Injection Point. | 23 |
| 14 | Impressions of 1% Polymer Solution Breakup (Flow Conditions same as in Figure 13). | 24 |
| 15 | Impressions of 2% Polymer Solution Breakup (Flow Conditions same as in Figure 13). | 25 |
| 16 | Impressions of 5% Polymer Solution Breakup (Flow Conditions same as in Figure 13). | 26 |

| | | |
|---|---|---|
| 17 | Breakup of 5% Polymer Solution in Coaxial Jet Facility, Outer Jet = 230 m/s, Inner Jet = 190 m/s, and Temperature 20°C. | 28 |
| 18 | Breakup of 5% Polymer Solution in Coaxial Jet Facility, Outer Jet = 230 m/s, Inner Jet = 190 m/s, and Temperature 70°C. | 29 |
| 19 | Breakup of 5% Polymer Solution in Coaxial Jet Facility, Outer Jet = 300 m/s, Inner Jet = 230 m/s. | 30 |
| 20 | Breakup of 5% Polymer Solution in Coaxial Jet Facility, Outer Jet = 300 m/s, Inner Jet = 230 m/s, and Temperature 70°C. | 31 |
| 21 | Drop Size Spectrum of Polymer Solution Breakup (See Figure 20 for captions). | 32 |
| 22 | Drop Size Spectrum (Volume Contribution) of Polymer Solution Breakup (See Figure 20 for captions). | 33 |

BLANK

# Aerodynamic Breakup of Polymer Solutions via Digital Image Processing Techniques

## 1. INTRODUCTION

The characterization and control of the aerodynamic breakup of liquids is important for many industrial applications. Among them: atomization of liquid fuels, paint sprays, explosive dissemination, post-crash aircraft fuel misting, etc. It is well known that a high relative air velocity causes the breakup of Newtonian liquids to extremely small drops. For some of the applications described above, this feature is undesirable because the fine drops may remain in the air for a long time and fail to impact the intended target, or form a large fireball due to ignitability of fine mist formed during an aircraft crash landing. To overcome this problem polymers are often added to modify liquid rheological properties[1,2]. Although many research efforts have been devoted toward Newtonian liquid breakup, little is known on the breakup of non-Newtonian fluids[3]. Because of the viscoelastic and time dependent behavior of many polymer solutions, highly non-spherical drops are formed during atomization which cannot be accurately characterized with conventional spray counting techniques[4]. Furthermore, drop size distributions of these sprays may not be assumed to be similar to those of typical Newtonian sprays, so that classical instrumentation relying on the existence of such a distribution may yield erroneous results. To study aerodynamic breakup of non-Newtonian polymer solutions eluding the difficulty of choosing a prior drop size distribution, JPL has developed a novel spray analysis system[5]. The system relies on the use of pulsed laser photographic and digital processing of the drop field pictures.

One of the experimental techniques used in the past to investigate viscoelastic breakup[3] employed impression cards. Due to complex rheological polymer properties, large errors can be introduced in relating the impressions to the actual drop dimensions in flight. To avoid this unknown error, a non-intrusive, laser-pulsed photographic technique to measure in-flight polymer solution breakup was employed. The photographic data were subsequently digitized and analyzed by image processing techniques. These results are discussed below.

## 2. EXPERIMENTAL APPROACH

### 2.1. Test Fluids.

The test fluid used in this study was diethylmalonate (DEM) with various concentrations of polymethyl methacrylate (PMMA) based polymer Acryloid K-125 as additive. To enhance the drop measurements 2% (w/v) Calco Oil Blue ZV was added to all solutions. The concentration of the polymer solutions ranged between 1-5% (w/v). The solutions were prepared by adding the polymer powder to 90% of the required amount of solvent and then allowing the suspension to stand undisturbed overnight. The balance of the solvent containing the dissolved dye was subsequently added. In the final step, the solutions were filtered through a 16 mesh screen. Limited tests were also performed with glycerol as a test solution.

## 2.2 Wind Tunnel Test Procedure.

The simulation of the aerodynamic breakup can be achieved by exposing the polymer solution to a high velocity air stream. To generate this airflow, two different facilities were employed.

### 2.2.1 Open Jet Wind Tunnel.

A free-jet flow of 12.7-cm-diameter with a maximum velocity up to 250 m/s was employed as shown in Figures 1 and 2. Polymer solutions were introduced at the jet center approximately one diameter downstream from the nozzle exit plane. The solution reservoir was pressurized up to 60 psi. A liquid jet of approximately 6 or 9 mm diameter was injected downstream into the high speed airflow through stainless steel tubing. The aerodynamic breakup process was studied at various locations downstream of the injection point. Provisions were also made for the liquid jet to impinge onto a paraboloidal, center body to obtain a sheet breakup as seen in Figures 1 and 2. Photographs were taken both at 40 cm and 240 cm downstream of the liquid injection point. Tests were run at room temperature and $60^{o}$-$70^{o}$C. Prior to DEM breakup studies, limited tests with glycerol were also performed.

### 2.2.2 Coaxial Jet Facility.

To provide increased in-flight relaxation of the polymer after its aerodynamic breakup, a coaxial jet nozzle as sketched in Figure 3 was constructed. Figures 4 and 5 show the photographs of this facility. The polymer solution was injected with air flowing on both sides of the annular liquid jet. The flow was directed downward towards the ground. By changing the stagnation pressure on each side, the polymer solution could be exposed to different shear conditions. High subsonic to supersonic air flow conditions could be independently attained in inner and annular outer jets. This facility had provisions to heat the polymer solution up to $100^{o}$C. The solution tank could be pressurized up to 100 psig. The breakup pictures were taken about 18 inches above the ground. This arrangement provided a 3.5m free-fall for polymer relaxation. To obtain increased droplet density at the imaging plane, it was desirable to keep outer annular jet flow velocity higher than the inside jet.

## 2.3 Flow Illumination and Photographic Techniques.

Photographing of droplets with sharp boundaries moving at speeds of up to 200 m/s in air requires exposure durations on the order of nanoseconds. Such intense short pulsed illumination was achieved with a ruby pulsed laser. Background illumination Q-switched technique as sketched in Figure 6 was employed. The pulsed laser illuminates a ground glass screen which serves as a background for the droplet field. The camera views the drops against this illuminated background. The plane of focus of the camera is located within the droplet field while the illuminated ground glass screen is out of focus. The ground glass screen diffuses the expanded incident laser beam, thus eliminating diffraction problems around droplet edges. The images of in-focus droplets thus appear very sharp.

Figure 1 Free-Jet Facility

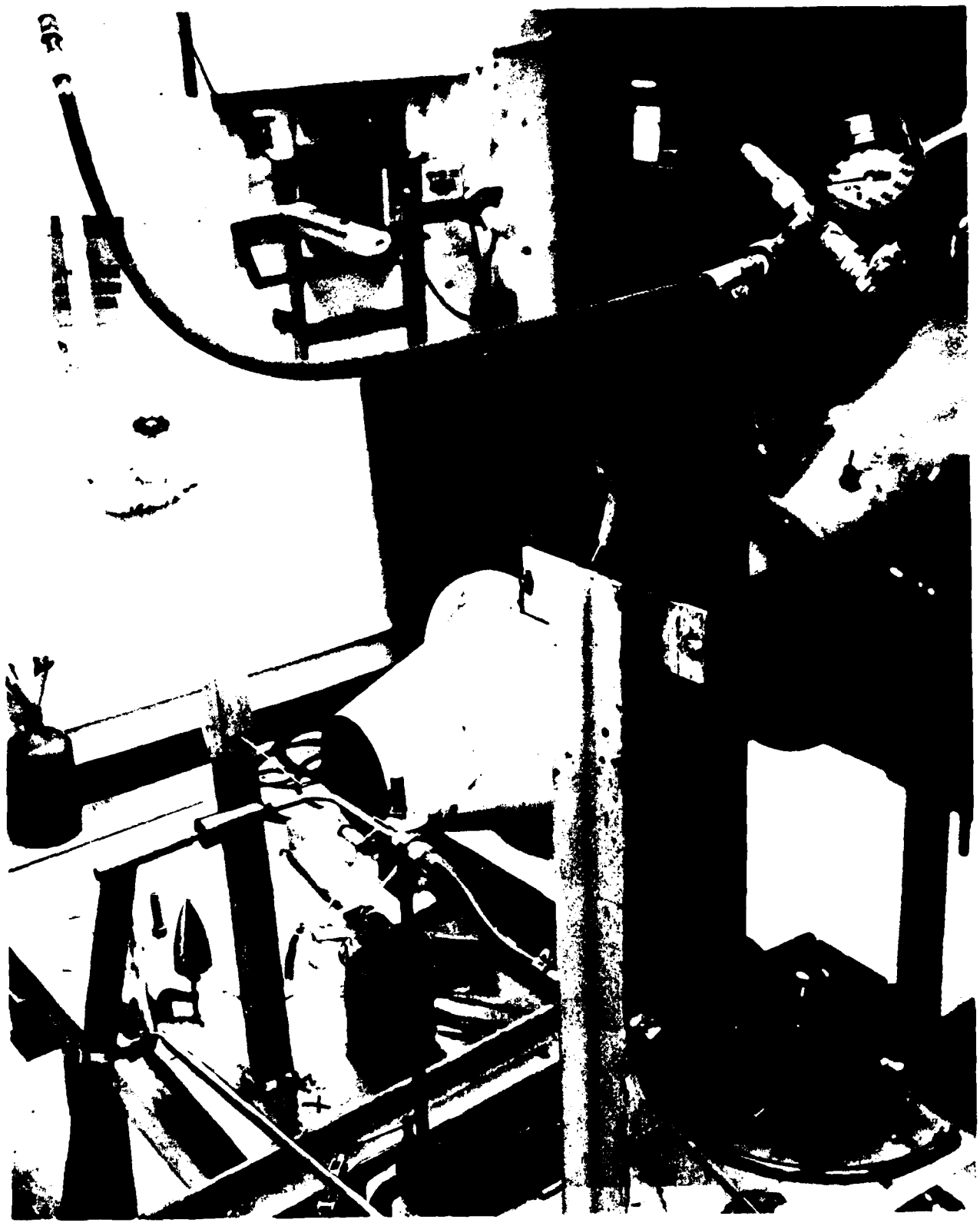

Figure 2 Free-Jet Facility

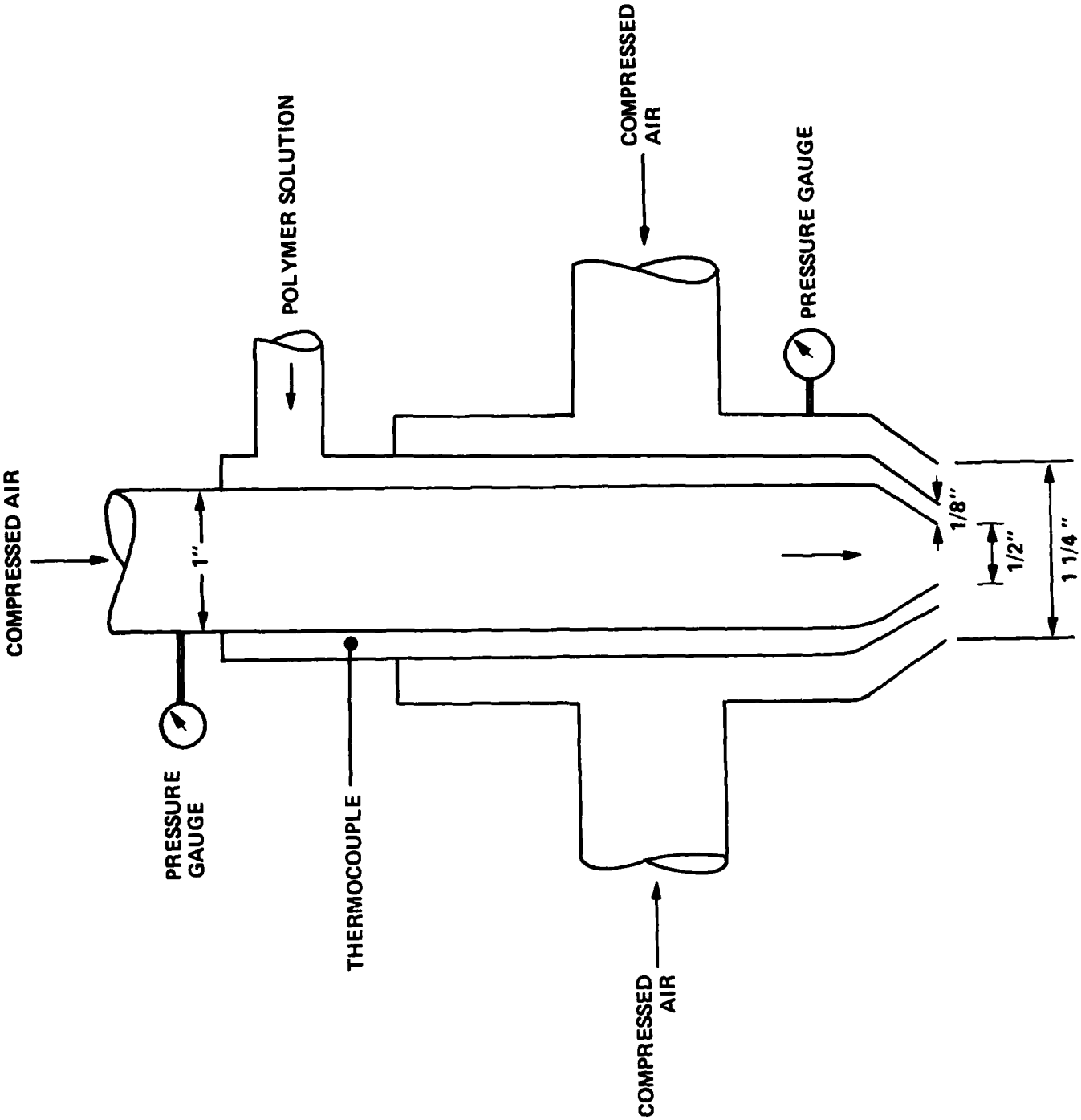


Figure 3 Sketch of Coaxial Jet Facility

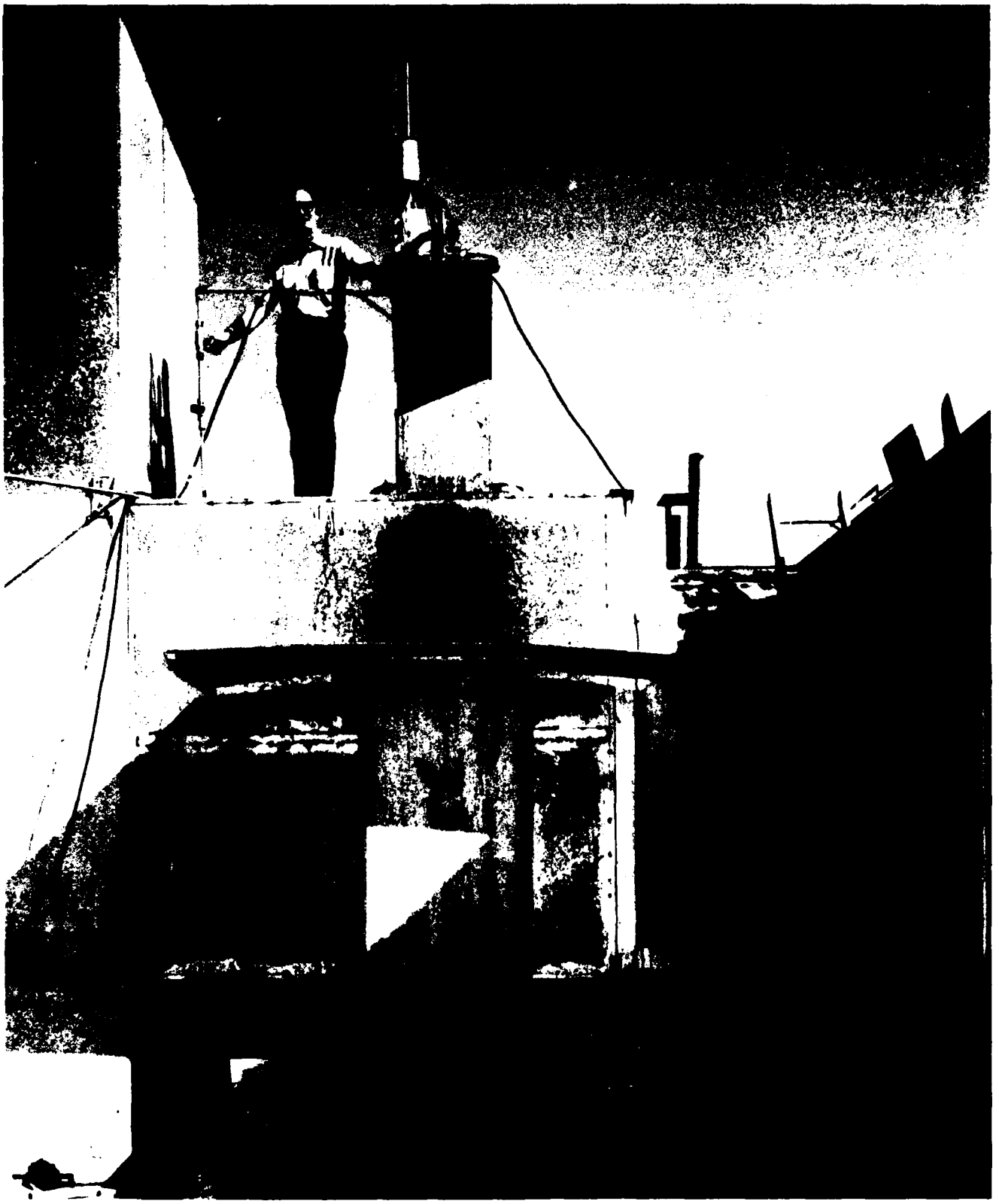

Figure 4 Coaxial Jet Facility

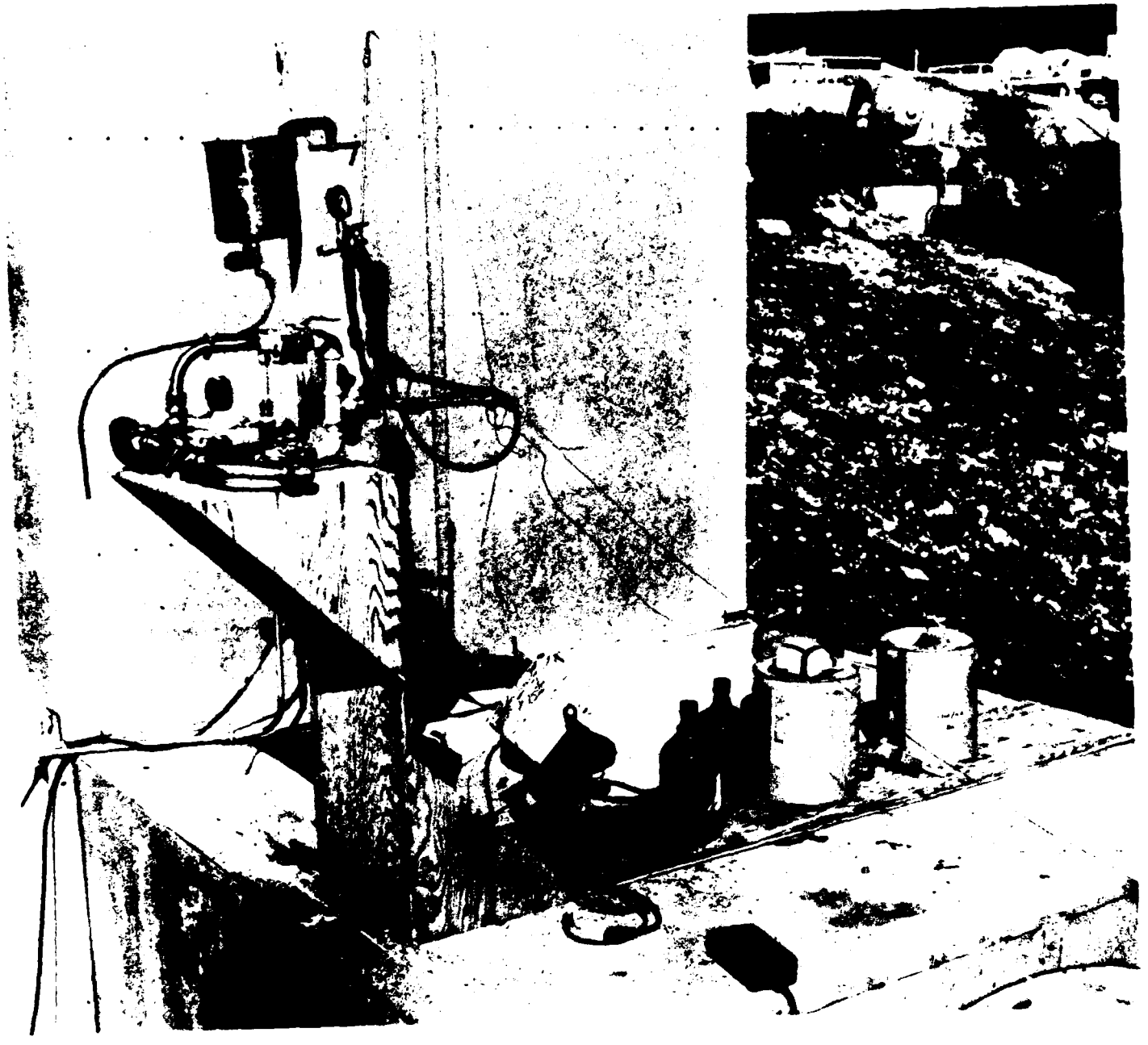

Figure 5 Close-up of Coaxial Jet Facility

## DROPLET PHOTOGRAPHIC SYSTEM

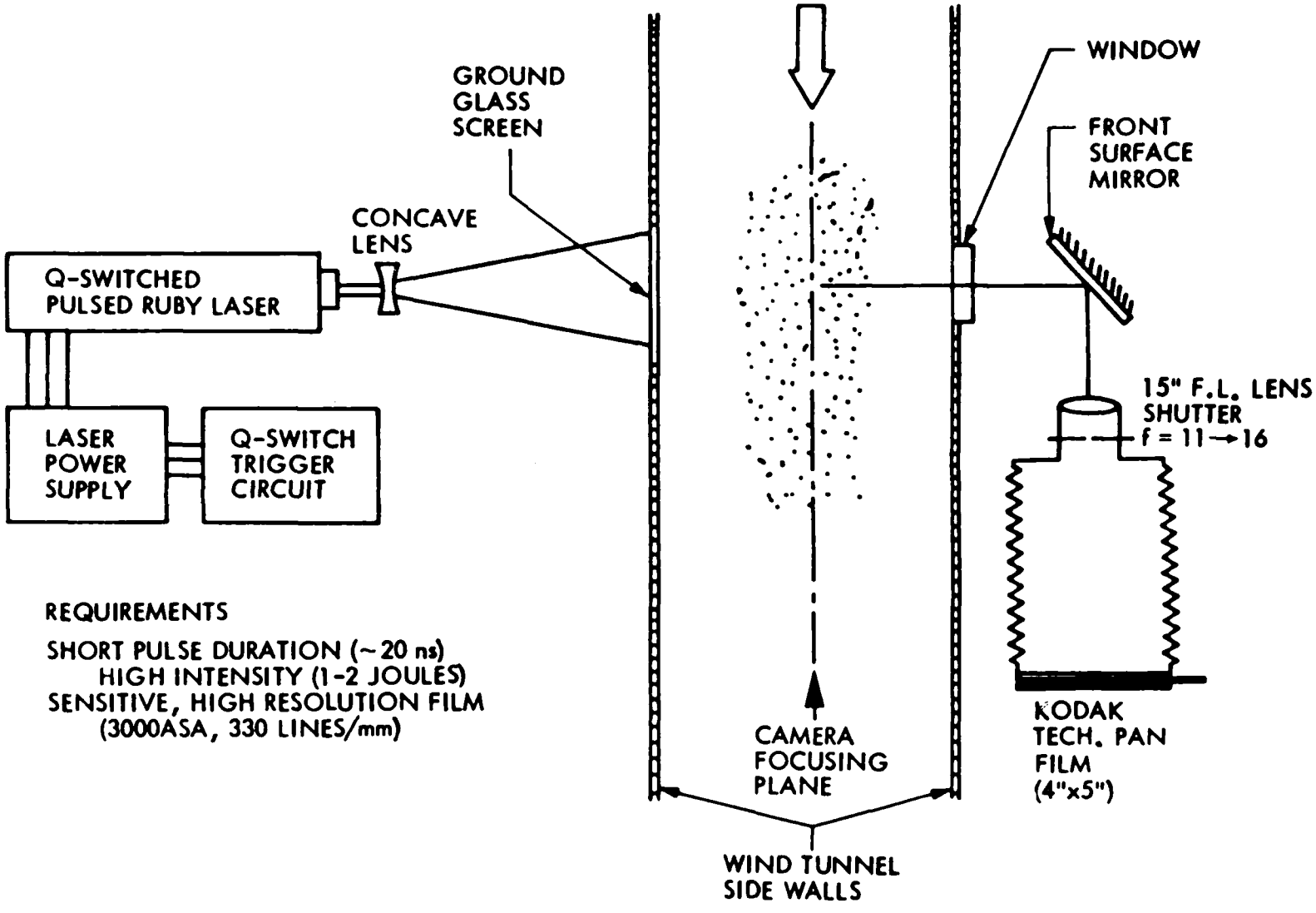


Figure 6 Schematic of Background Illustration and Photographic Technique.

Kodak Technical Pan film was used for the photographic system because of its high resolution and its sensitivity to light in the red portion of the visible spectrum. A red filter was also fitted over the objective to eliminate interferences from ambient light.

## 2.4 Digital Image Analysis.

Analysis of the spray images is accomplished with the system described in the Appendix. This system is operational on a PDP 11/34 mini-computer, working in conjunction with a DeAnza ID5400 video processor. The hardware package also includes a video camera and A/D converter for image digitization. Software for image enhancement, filtering, classification, and shape analysis is available and residing in the host computer libraries.

During droplet analysis out-of-focus droplets will also show up in the photographs with fuzzy boundaries. However, during subsequent digital analysis of photographs, only the droplets with sufficiently (as specified by the operator) sharp edges are included in statistics. Another potential problem with the technique is superposition of the images of two or more drops which may be accounted for as a single large drop in the subsequent analysis. Here too, safeguards have been built into the software to exclude such drops in the analysis by determination of a shape factor.

# 3. RESULTS AND DISCUSSIONS

## 3.1 Free Jet.

Digitally enhanced in-flight breakup of glycerol at 250 m/s airflow taken 40 cm downstream of the injection point is shown in Figure 7. As expected, breakup into droplets was observed immediately downstream of the injection point. However, DEM containing PMMA polymer breakup was quite different in this region as can be seen in Figures 8-11 for polymer concentrations of 0.5%, 1%, 2%, and 5%. These laser shadowgraphs were taken approximately 40 cm from the injection point, freestream velocity of 250 m/s (except 11B - where freestream velocity was 200 m/s) and 20$^{o}$C solution temperature. These photographs were digitized and processed to enhance the image sharpness by removing the out-of-focus ligaments and by improving the boundary intensity of in-focus ligaments. As is evident, the breakup of the viscoelastic polymer solution in near-field region is not into well defined droplets but rather in sheets and ligaments. To improve the breakup, the solution was heated to about 100$^{o}$C in the tank. Figure 12 shows the breakup of 5% PMMA. The solution temperature was approximately 68$^{o}$C at the injection point. No significant difference in breakup pattern was observed.

During the course of in-flight breakup studies, droplet impressions on cards 12m downstream were also recorded. The photographs in Figures 13, 14, 15, and 16 are typical examples of these impressions at PMMA concentrations of 0.5%, 1%, 2%, and 5%. It is evident from these photographs that with increased flight time, significant relaxation/recoiling of polymer ligaments, as observed in near-field photographs 7 through 12, takes place. Due to extremely dilute density of the droplets 12m downstream of the injection point, no attempt to photograph

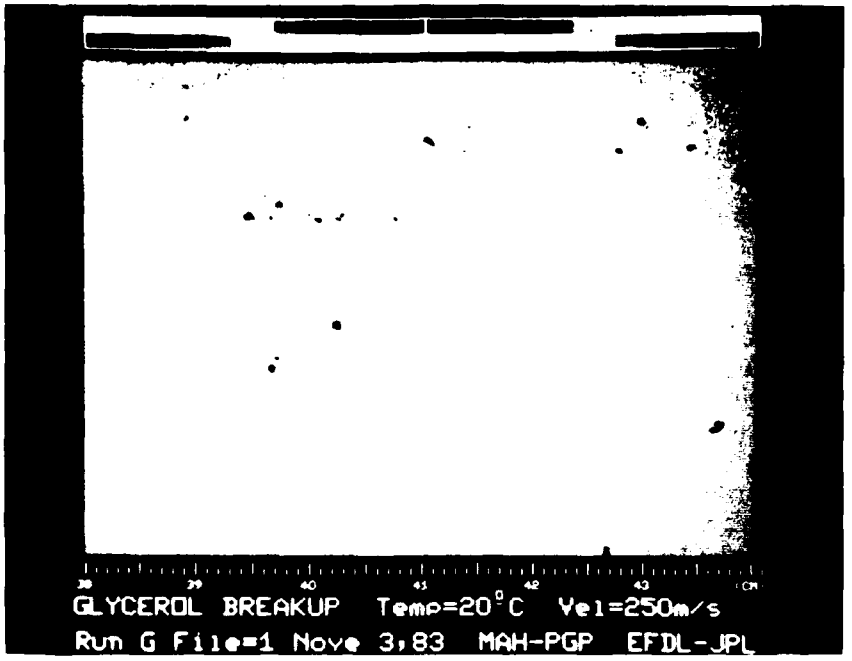


Figure 7 Image enhanced breakup of Glycerol (see figure captions).

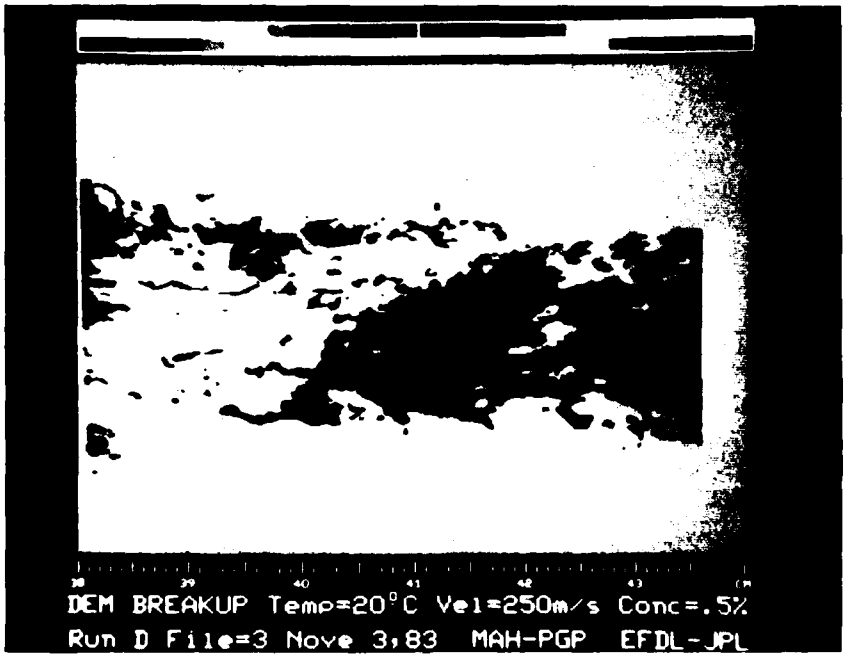


Figure 8 Near-Field breakup of 0.5% polymer solution.

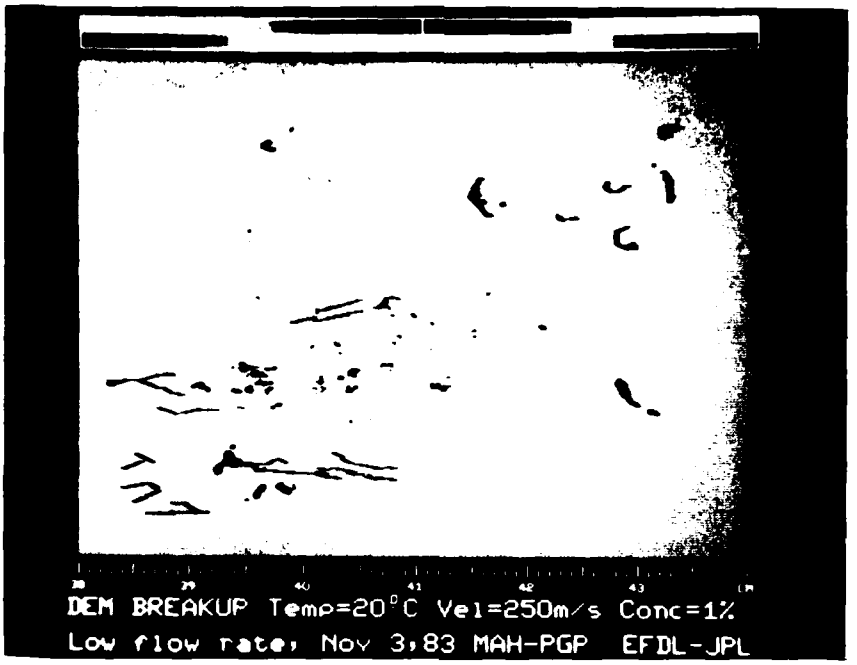


(A)


(B)

Figure 9 A-B Near-Field breakup of 1% polymer solution.

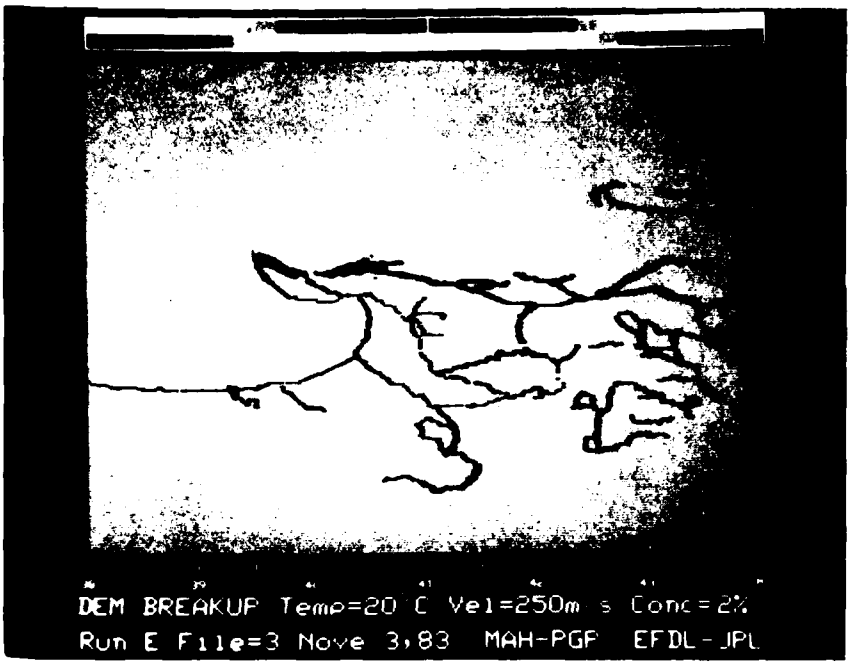


**Figure 10 Near-Field breakup of 2% polymer solution.**

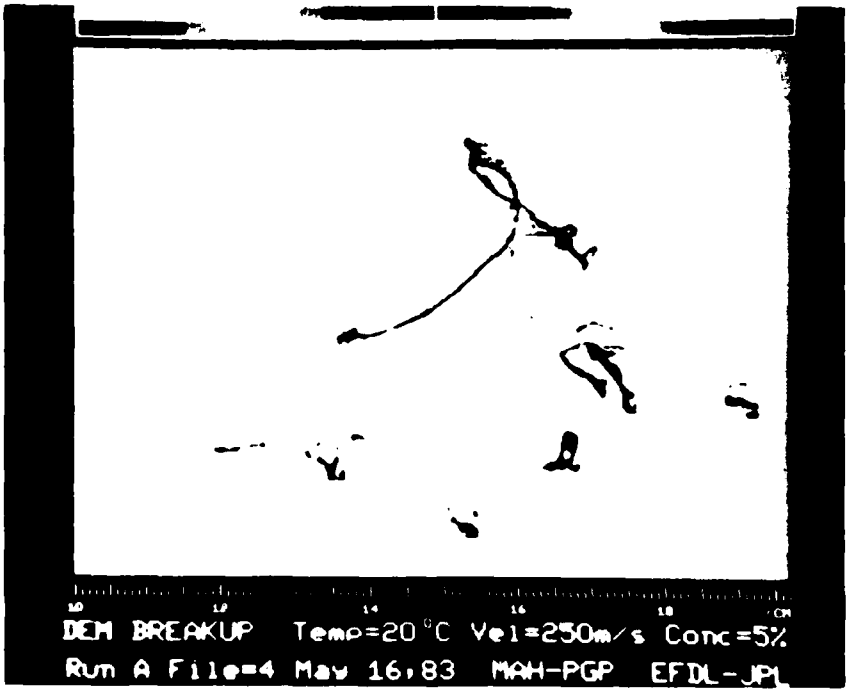


(A)

Figure 11 Near-Field breakup of 5% polymer solution.

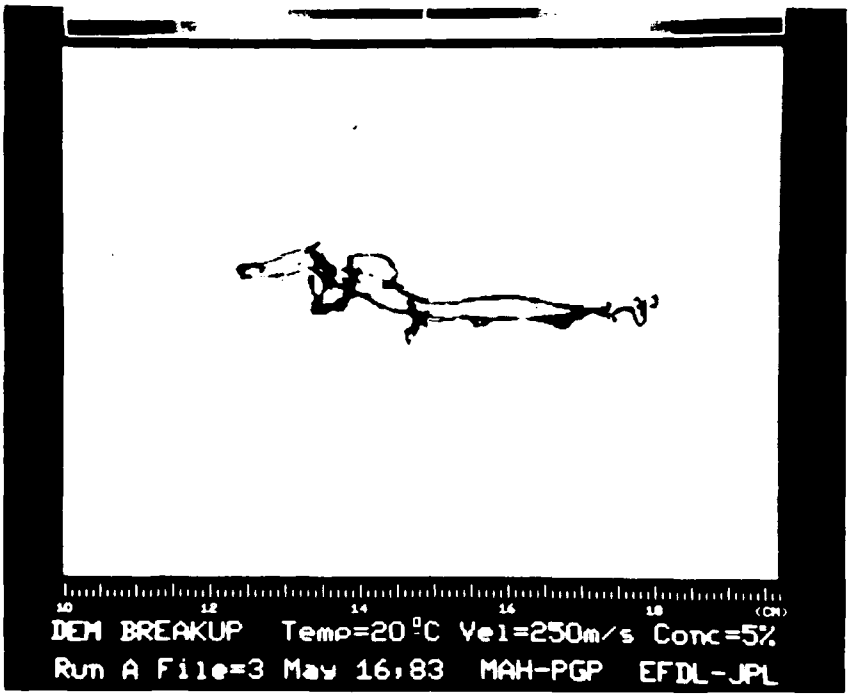


(B)

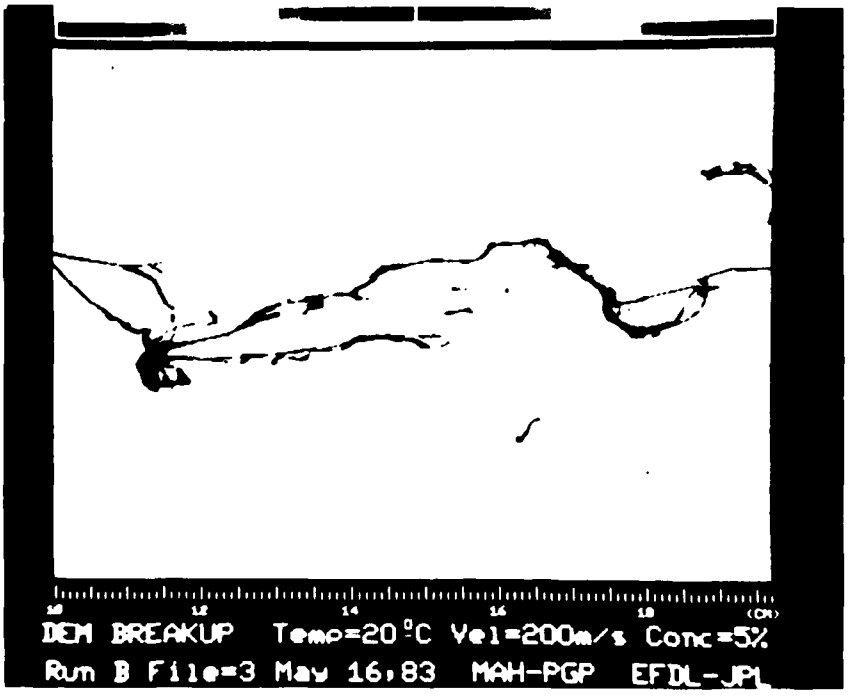


(C)

Figure 11 A,B,C Near-Field breakup of 5% polymer solution. (Continued)

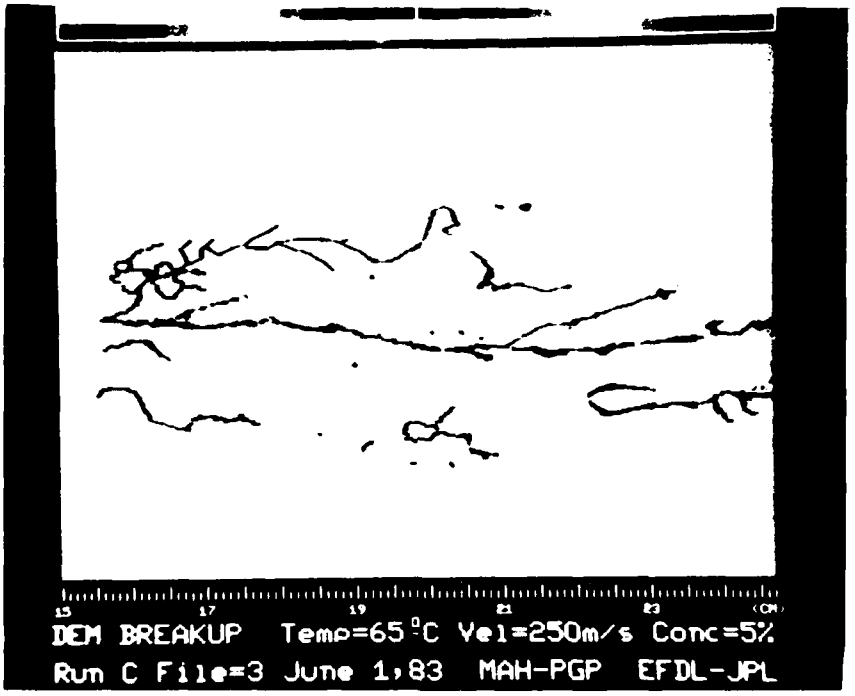


(A)

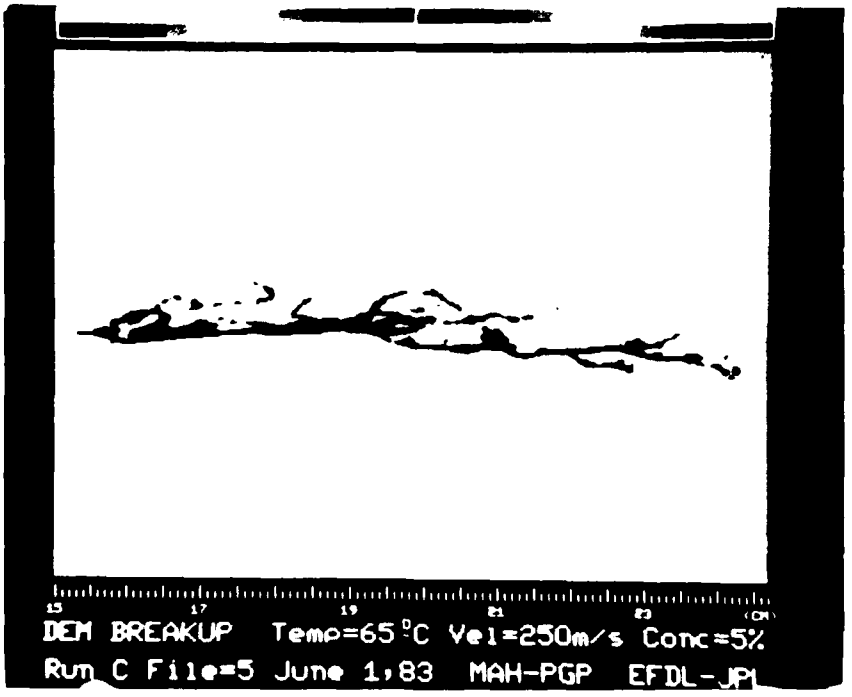


(B)

Figure 12 A-B Influence of temperature on near-field breakup of 5% polymer solution.

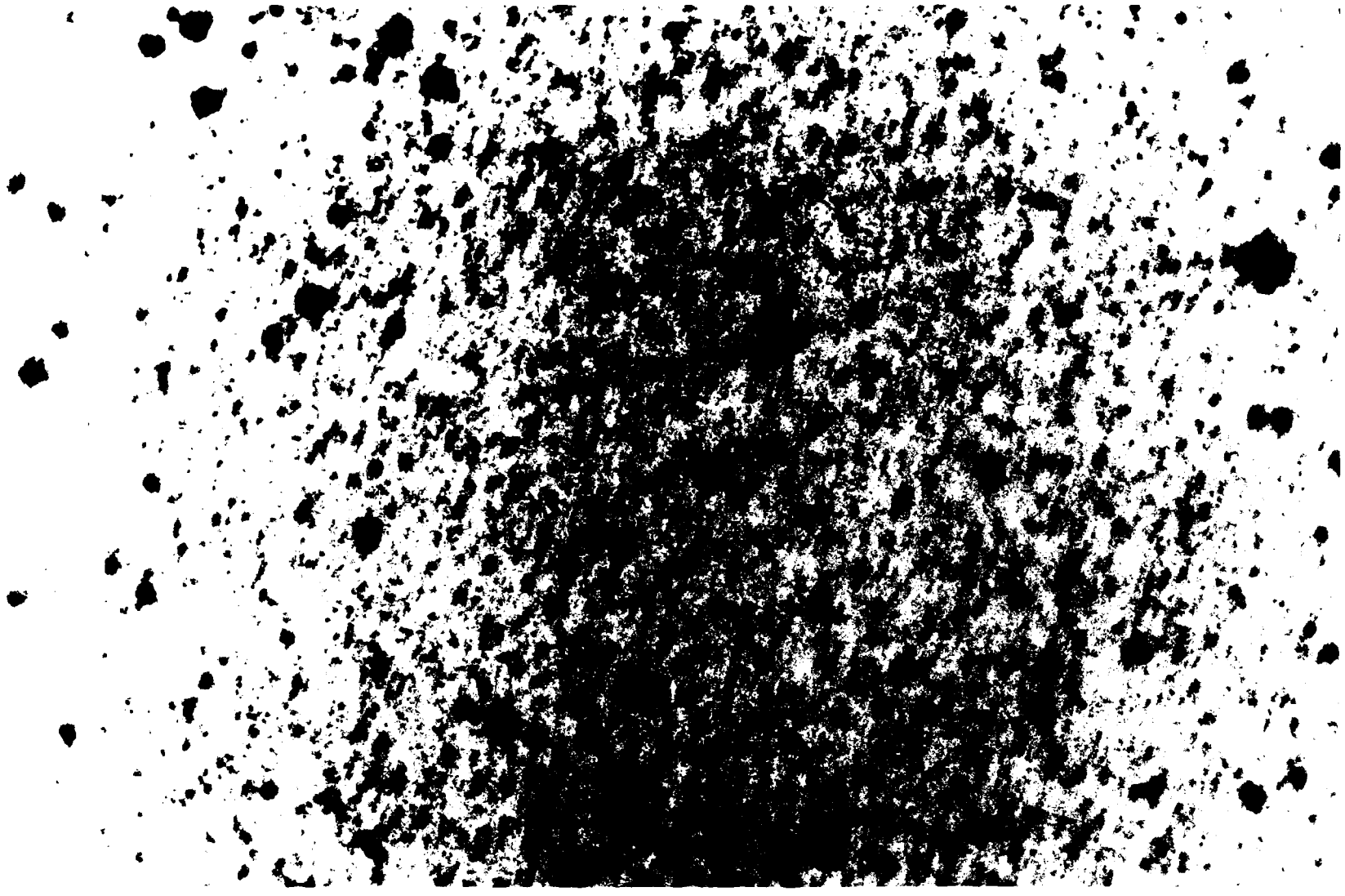

Figure 13 Impressions of 0.5% polymer solution breakup at temperature 20°C, freestream velocity 250 m/s, and 12m downstream from injection point.

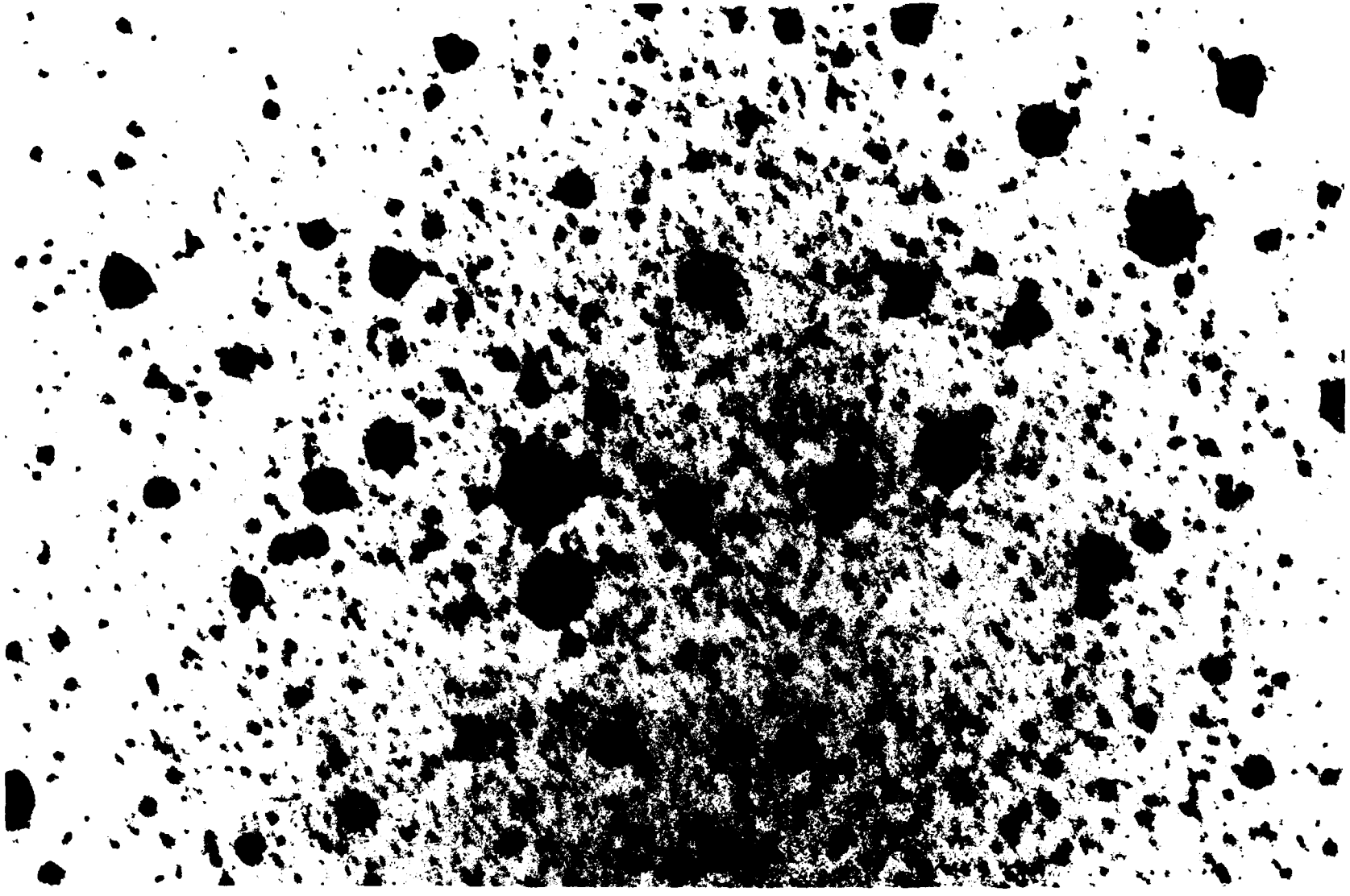

Figure 14 Impressions of 1% polymer solution breakup (flow condition as in Figure 13).

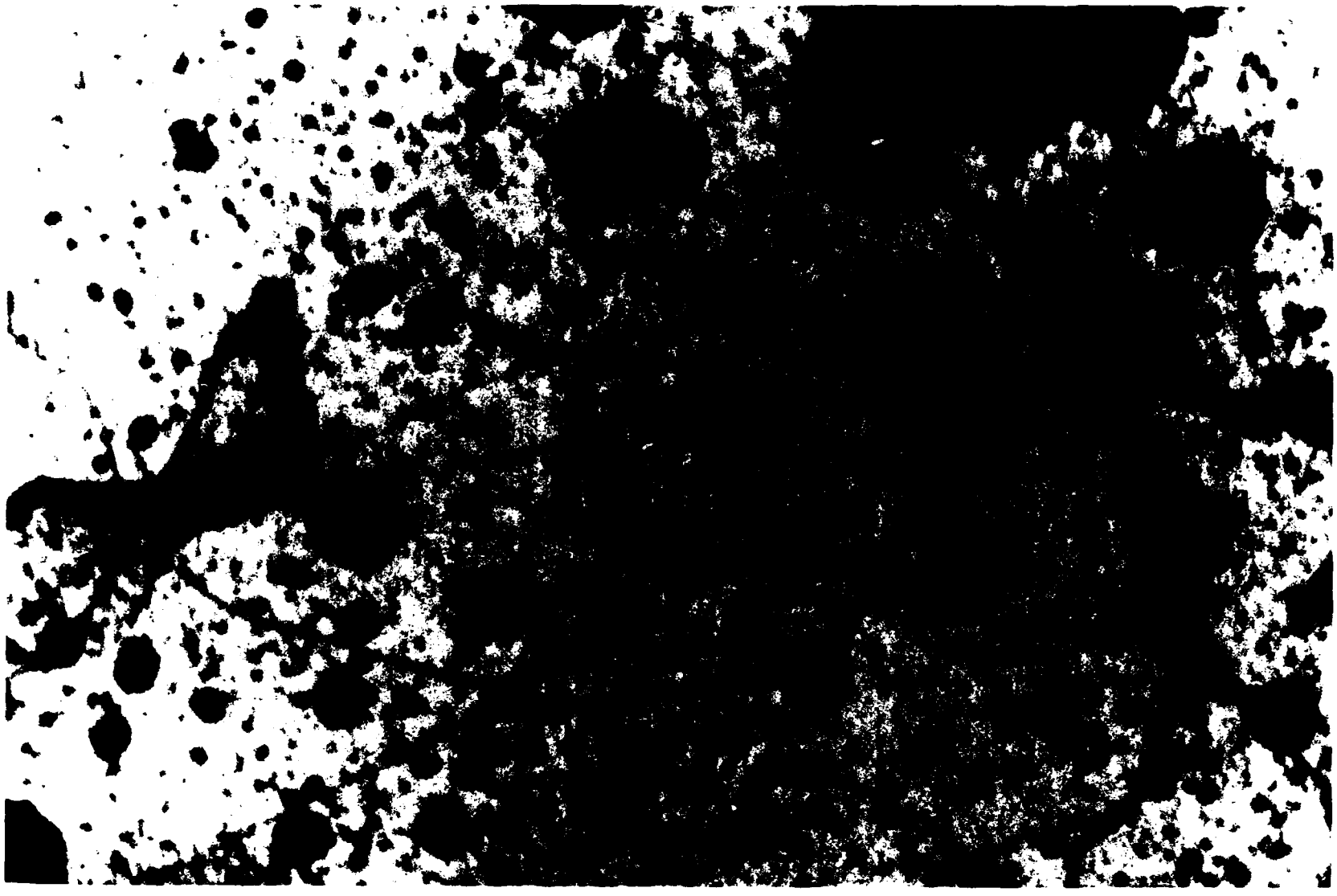

Figure 15 Impression of 2% polymer solution breakup (flow conditions as in Figure 13).

Figure 16 Impressions of 5% polymer solution breakup (Flow conditions same as in Figure 13).

these drops in-flight were taken. Instead, a coaxial jet facility was built and the results obtained are discussed next. This facility not only provided aerodynamic breakup but also enough residence time for polymer to recoil to its final shape.

## 3.2 Coaxial Jet.

Breakup of polymer at two different pressure settings and liquid temperatures was performed. The solution concentration was 5% PMMA in diethylmalonate. In Figure 17, the outer air velocity was 230 m/s and the inner velocity was 190 m/s. Figure 18 shows the breakup under the identical flow conditions but the solution temperature was raised from 20°C to 70°C. Marked improvement in breakup pattern is evident with increased temperature.

Figures 19 and 20 show breakup of 5% polymer concentration at 20°C and 70°C respectively where the outer and inner jet velocities were 300 and 230 m/s. The photograph shown in Figure 20 was digitized and the drop statistic data are shown in Figures 21 and 22. Figure 20 shows the arithmetric droplet statistics whereas their volumetric contribution is shown in Figure 21. The statistical data are also tabulated in Table 1.

# 4. CONCLUSIONS

The present study has demonstrated successfully the applicability of laser pulsed photographic techniques, combined with digital image analysis to quantify the in-flight aerodynamic breakup of non-Newtonian liquids. Large dynamic range of non-spherical drops from few microns to several millimeters can be easily analyzed where commercially available current light scattering techniques cannot be reliably applied. The imaging software developed is capable of distinguishing out-of-focus and in-focus drops retaining the latter for size distribution. During the second phase of the research, the unique coaxial jet experimental setup developed for this task combined with digital image analysis techniques will be applied to relate the material properties to precise drop size data under known aerodynamic breakup conditions. Such information will greatly assist in material evaluation for explosive aerodynamic breakup of polymer solutions.

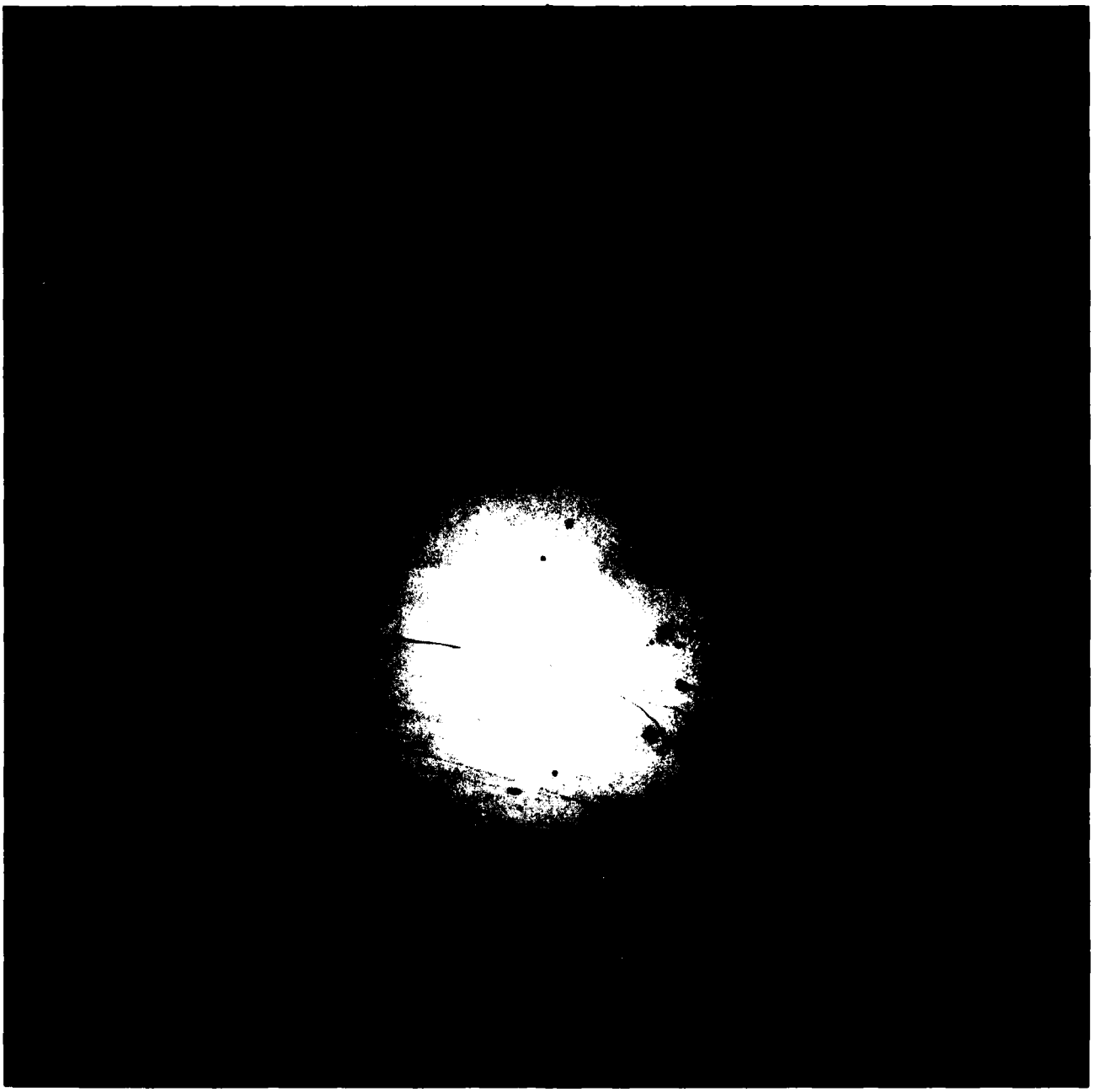

Figure 17 Breakup of 5% polymer solution in Coaxial Jet Facility, Outer Jet = 230 m/s, Inner Jet = 190 m/s, and temperature 20°C.

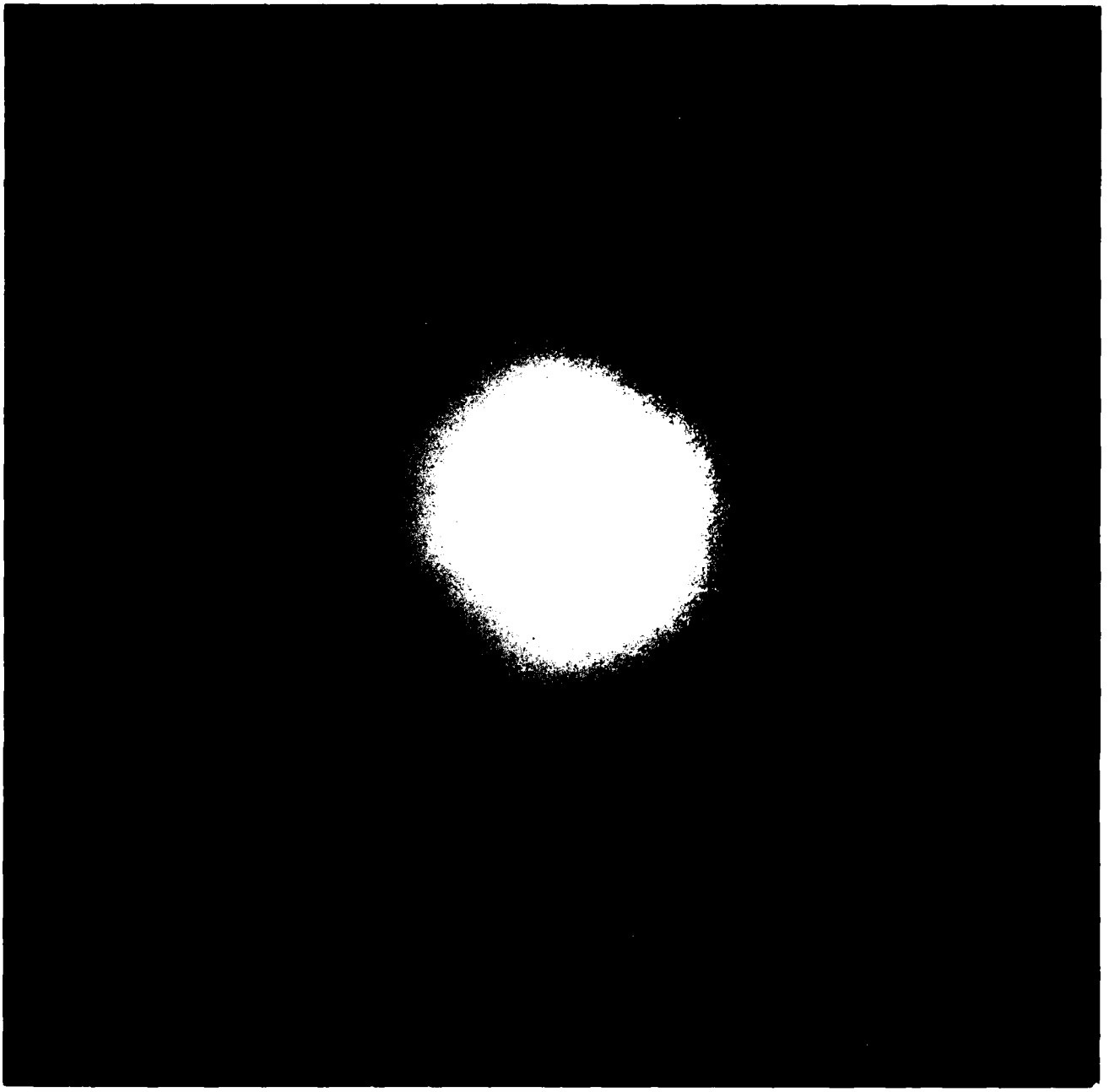

Figure 18 Breakup of 5% polymer solution in Coaxial Jet Facility, Outer Jet = 230 m/s, Inner Jet = 190 m/s, and temperature 70°C.

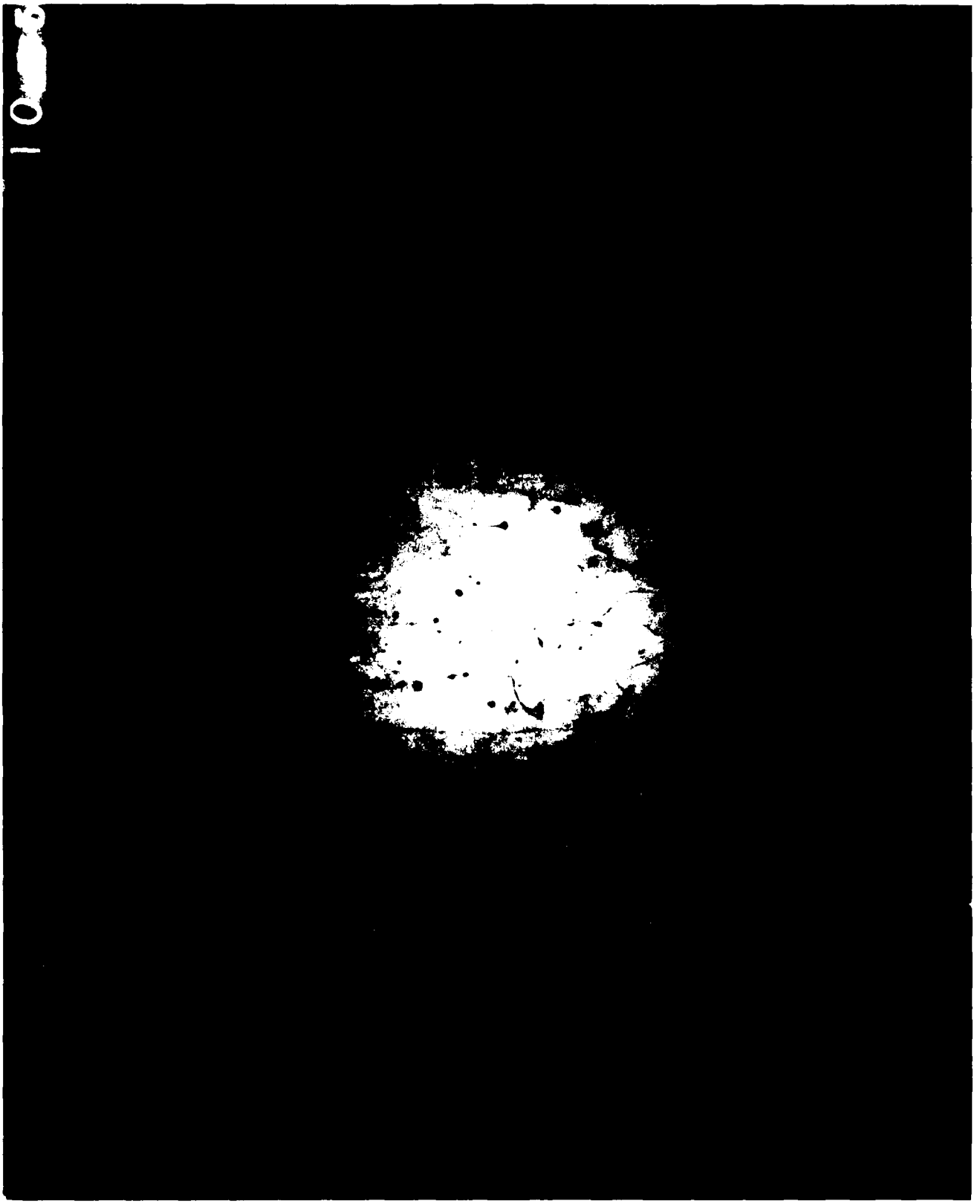

Figure 19 Breakup of 5% polymer solution in Coaxial Jet Facility, Outer Jet = 300 m/s, Inner Jet = 230 m/s.

Figure 20 Breakup of 5% polymer solution in Coaxial Jet Facility, Outer Jet = 300 m/s , Inner Jet = 230 m/s, and temperature 70°C.

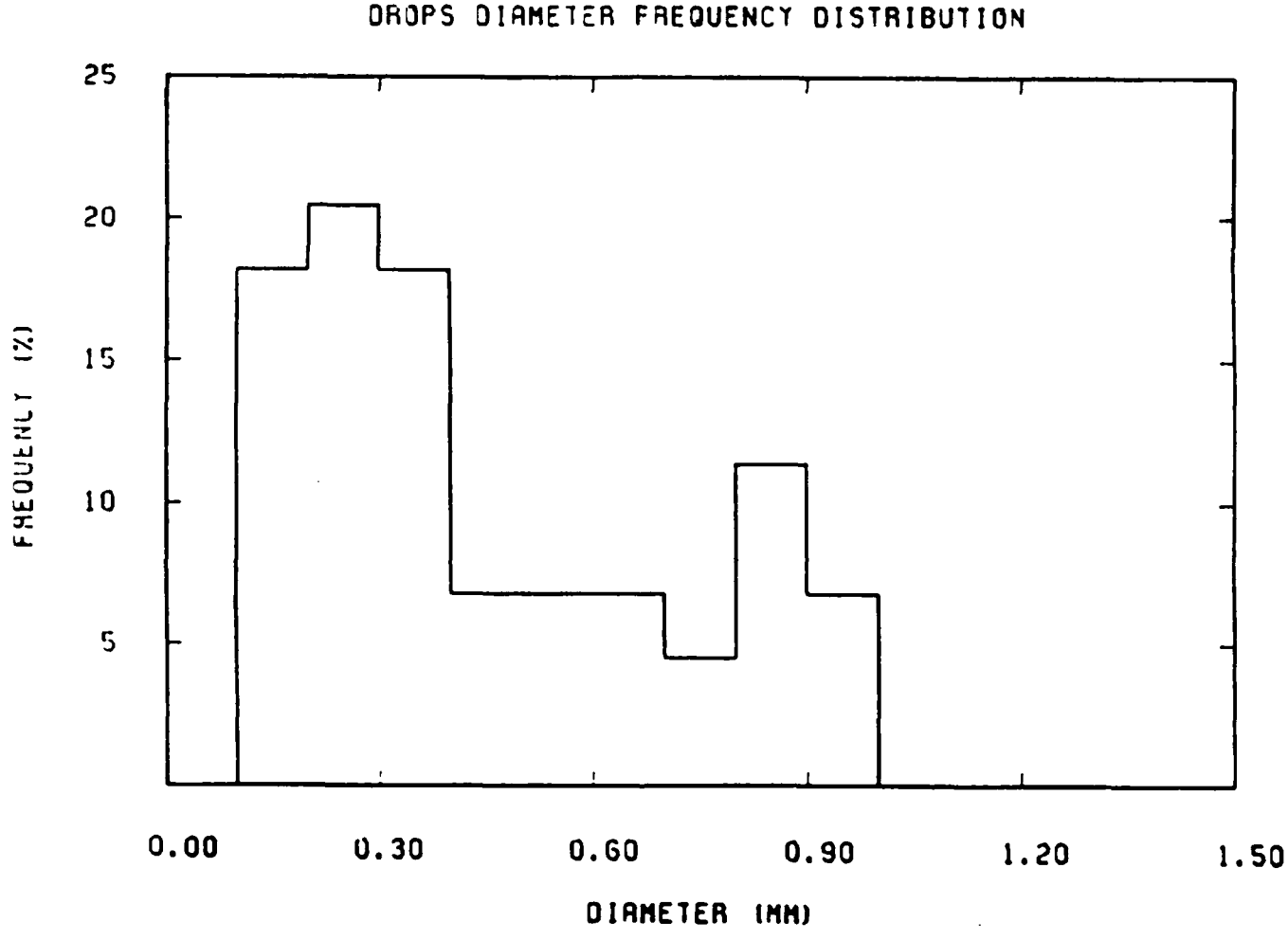


Figure 21 Drop size spectrum of polymer solution breakup (see Figure 20 for captions).

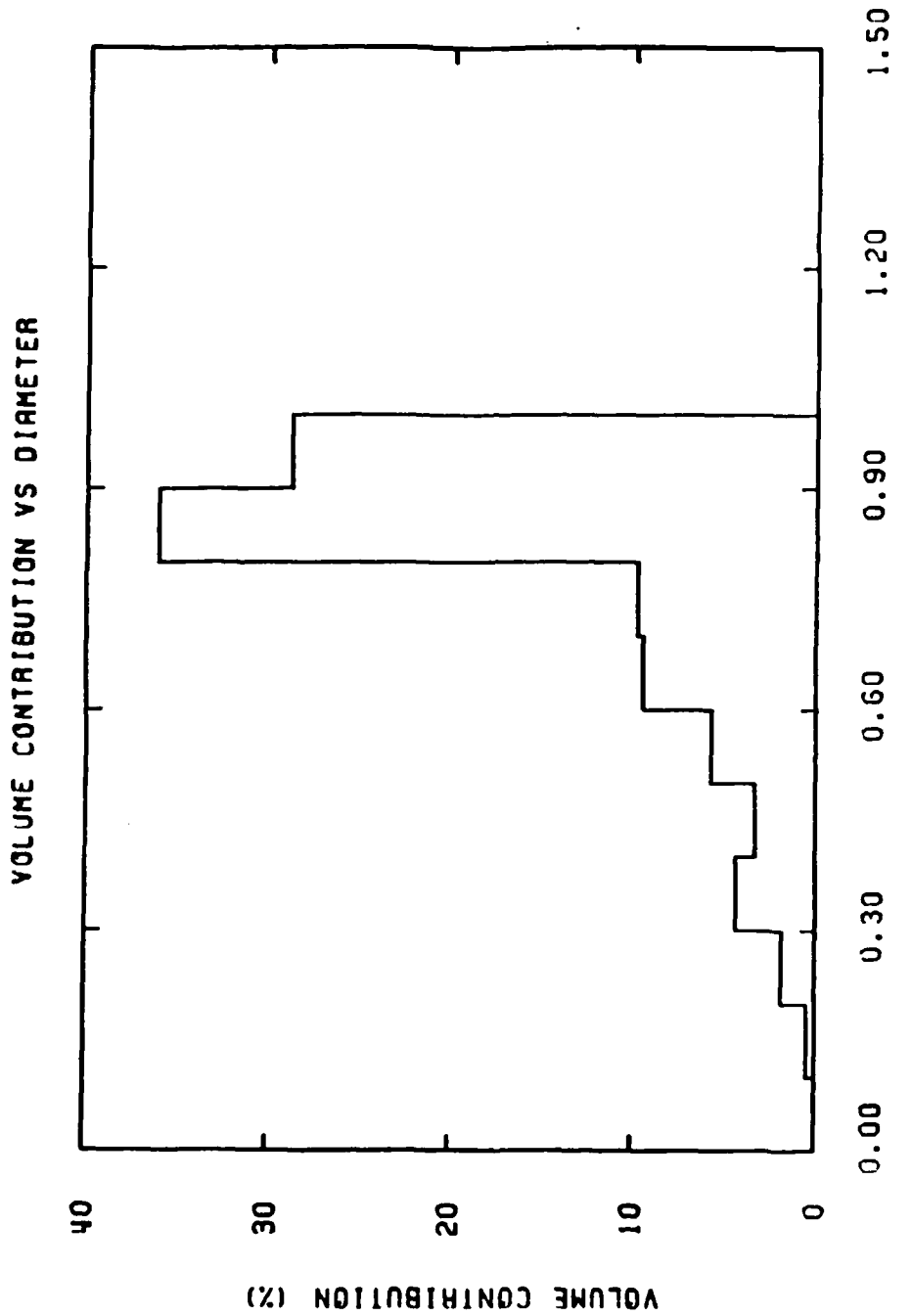


Figure 22 Drop size spectrum (volume contribution) of polymer solution breakup (see Figure 20 for captions).

## Table 1

## STATISTICAL DATA

Outside Nozzle Velocity = 300 m/s

Inside Nozzle Velocity = 230 m/s

Polymer Concentration = 5%

Polymer Temperature = 70°C

### DROPS SIZE STATISTICS

Sample Size = 44 Drops

**MEAN DIAMETERS**

Mean diameters are expressed according with the following notation:

$$D_{pq} = \left[ \frac{\sum n_i D_i^{\,p}}{\sum n_i D_i^{\,q}} \right]^{\frac{1}{p-q}}$$

Length Mean Diameter ..... D10 = .36 mm

Standard Deviation (length) ..... StD = .25 mm

Area Mean Diameter ..... D20 = .52 mm

Volume Mean Diameter ..... D30 = .57 mm

Sauter Mean Diameter ..... D32 = .72 mm

Volume Distribution Mean Diameter ..... D43 = .77 mm

**MEDIAN DIAMETER**

The median diameter is that diameter which divides the spray size distribution into two equal portions by number, length, surface, etc.

Length Median Diameter ..... DL.5 = .36 mm

**DISTRIBUTION LIMITS**

Diameter biggest drop .....Dmax = .94 mm

Diameter smallest drop .....Dmin = .16 mm

**DROPS CIRCULARITY**

Circularity is defined as the ratio

$$\text{Circularity} = \text{perimeter}^2/4\pi\,\text{area}$$

Mean Circularity ..... 1.39

Standard Deviation ..... .29

## LITERATURE CITED


1. Sarohia, V., AIAA Paper No. 81-1422. Fundamental Studies of Antimisting Fuels, Presented at the AIAA/SAE/ASME, 17th Joint Propulsion Conference, Colorado Springs, Colorado, July 27-29, 1981.

2. Hoyt, J.W., Taylor, J.J., and Runpe, C.D., "The Structure of Jets of Water and Polymer Solutions in Air," Journal of Fluid Mechanics, Vol. 63, 635-640 (1974).

3. Matta, J.E., and Tytus, R.P. "Viscoelastic Breakup in a High Velocity Airstream," Journal of Applied Polymer Science, Vol. 27, 397-402 (1982).

4. Fleeter, R., Toaz, R.D., and Sarohia, V., Application of Digital Image Analysis Techniques to Antimisting Fuel Spray Characterization, presented at ASME, 1982 Winter Annual Meeting, Phoenix, Arizona, 82-WA/HT-23.

5. Hernan, M.A., Parikh, P., and Sarohia, V., Droplet Field Visualization and Characterization via Digital Image Analysis, to be presented at International Symposium on Fluid Control and Measurement, Tokyo, 1985, September 2-6, 1985.

BLANK

## APPENDIX

## IMAGE PROCESSING SYSTEM DESCRIPTION

### A.1 System Architecture.

Processing system architecture is depicted by Figure A-1. Image acquisition, display and processing has been performed by a De-Anza ID-5400 image processing system. The hardware package incorporates a vidicon and power supply for analogue image formation, three image refresh random access memory channels, RAM, digital video array processor, and color video display. The analogue signal from the video camera can be digitized by an A/D converter and fed directly to the array processor which in turn controls the data flow and writes the data into one of the memory planes at a rate of 30 frames/sec. The digitization process converts each picture into a 512x512 matrix elements (pixels). Each pixel is one byte number (256 resolution level) representing the average optical density in a elementary cell, the size of which dictates the spatial resolution of the system. While digitization can proceed at video rates of 30 frames per second, a program is used which creates one digital frame from the average of 64 consecutive digitized frames. Thus, the image formed has low level of random noise caused by the vidicon and the digitizer electronics. The digitized image information is then stored on a mass-storage device for further off-line processing.

Software residing in the host computer (PDP 11/34) operates through a direct memory access, DMA, interface through which the PDP-11 sends and receives information from the video processor registers or from the RAM channels via a driver program. The vidicon image digitization, averaging and storage capability is part of this DMA interface software.

To study a spray picture, the negative is mounted on a flat light table and the vidicon is focused in that plane. Magnification onto the vidicon is then adjusted so that digital resolution is equated with the photographic one. The negative is scanned at wide horizontal and vertical increments so that sampling produces a mosaic of digital subimages covering the entire area of the spray. Alternatively, data may be derived, for example, at only one specific location clustering subimages about the region of interest. The computer operator manipulates the vidicon and light table interactively with the computer to follow the desired sampling strategy.

### A.2 Software Description.

Fundamental to the image processing phase of the research is the detection scheme for individual drops in the image. The main goal is to detect drops with a brightness profile characterized by relatively sharp gradients at the drops edges and nearly constant brightness values throughout the drops interior.

A standard approach to segmenting an image containing two principal brightness values, light and dark, is to examine the histogram of gray levels that are present in the picture. If the histogram is strongly bimodal one can attempt to segment the picture by thresholding it at a level between the histogram peaks. However, the height of each peak in the histogram is proportional to the area of the corresponding region in the scene. If the area

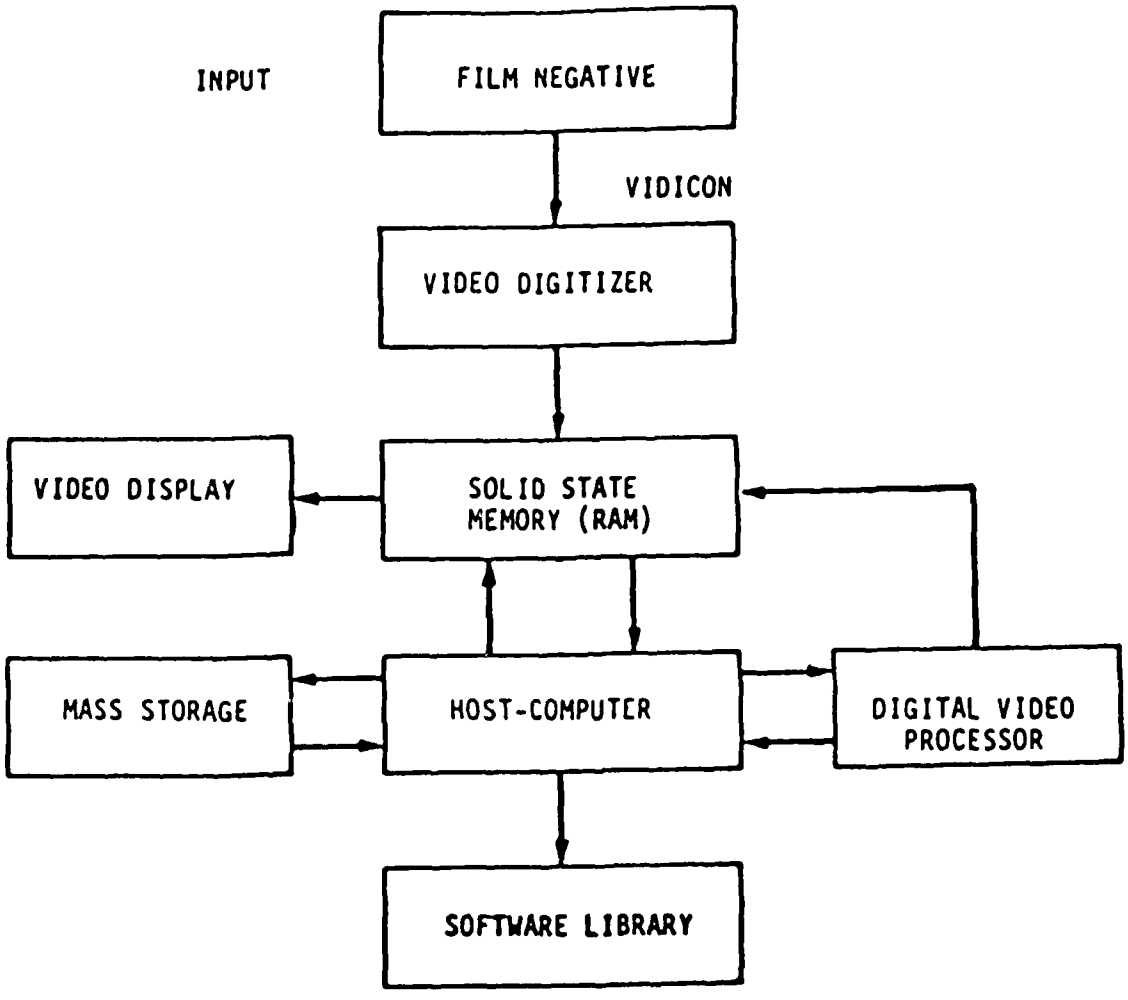


Figure A.1 Digital Image Processing System Architecture



APPENDIX

of one of the regions (e.g., background) is appreciably greater than the area of all the drops combined, the bimodality will not appear too clear. This situation may arise if we try to analyze a relatively dilute spary. In this case, a modification has to be included in our analysis consisting of computing the histogram only at the points where the brightness gradient is above a certain threshold.

Using such modified histogram based brightness thresholding, this operation will give rise to a classified image with regions of above threshold and below threshold points. By scanning the threshold classified image, in raster mode, adjoining pixels can be combined to define one dimensional droplet segments. For succeeding lines, adjoining segments are connected to represent a single, two dimensional drop. As each drop is completed its perimeter and area are computed, and the equivalent diameter (the diameter of a sphere with the same cross-sectional area as the drop) is calculated.

It should be noted that this process is sensitive to certain kinds of pictorial noise. For example, single noise points which differ from their surrounding will qualify as spot-like objects and will affect the final statistics. If this kind of noise is known to be present a priori, the size estimation algorithm should be able to reject any element whose size is below a certain minimum resolution limit.

It should also be noted that the drop detection algorithm does not assume that the spots are circle-like. Elongated elements associated with drops superimposed will, sometimes appear on the image. To exclude these situations, the algorithm performs a shape analysis step in which the measured perimeter is compared with the enclosed area and when this comparison is very different from that for a circle, a flag can be activated to reject this element.

Finally, in order to reject drops with fuzzy boundaries (out-of-focus) but containing regions of the same brightness level as an in-focus drop, another test is included in the algorithm. In this test, the number of points in the drop boundary where the brightness gradient is sharp enough is compared with the number of boundary points in the brightness thresholded image of the same drop. If the first number is much smaller than the second, the corresponding drop is considered out-of-focus and rejected in further analysis.

END

DTIC

9-86